



OPEN

Magnetic resonance T1w/T2w ratio and voxel-based morphometry in multiple system atrophy

S. Ponticorvo¹, R. Manara², M. C. Russillo¹, R. Erro¹, M. Picillo¹, G. Di Salle³, F. Di Salle¹, P. Barone¹, F. Esposito⁴ & M. T. Pellecchia¹✉

Diagnosis of multiple system atrophy (MSA) may be improved by using multimodal imaging approaches. We investigated the use of T1-weighted/T2-weighted (T1w/T2w) images ratio combined with voxel-based morphometry to evaluate brain tissue integrity in MSA compared to Parkinson's disease (PD) and healthy controls (HC). Twenty-six patients with MSA, 43 patients with PD and 56 HC were enrolled. Whole brain voxel-based and local regional analyses were performed to evaluate gray and white matter (GM and WM) tissue integrity and mean regional values were used for patients classification using logistic regression. Increased mean regional values of T1w/T2w in bilateral putamen were detected in MSA-P compared to PD and HC. The combined use of regional GM and T1w/T2w values in the right and left putamen showed the highest accuracy in discriminating MSA-P from PD and good accuracy in discriminating MSA from PD and HC. A good accuracy was also found in discriminating MSA from PD and HC by either combining regional GM and T1w/T2w values in the cerebellum or regional WM and T1w/T2w in the cerebellum and brainstem. The T1w/T2w image ratio alone or combined with validated MRI parameters can be further considered as a potential candidate biomarker for differential diagnosis of MSA.

Multiple system atrophy (MSA) is an adult-onset progressive neurodegenerative disorder featured by autonomic failure, parkinsonism and cerebellar ataxia with a prevalence of about 5 cases per 100,000. Oligodendroglial cytoplasmic inclusions consisting of misfolded α -synuclein are required for a definite diagnosis of MSA on postmortem examination¹. Neuronal loss, pathologic inclusions, iron accumulation and reactive astrogliosis are observed in the striatonigral and olivopontocerebellar systems^{2,3}. MSA can be clinically classified into the parkinsonian variant (MSA-P) and the cerebellar variant (MSA-C) based on the predominant motor features which is dependent on the distribution of pathology within the basal ganglia and cerebellum¹. However, the predominant motor features can change with time and the variability of the severity and regional distribution of pathological process accounts for a spectrum of disease.

The differential diagnosis between MSA, particularly the parkinsonian subtype, and Parkinson's disease (PD), the most frequent α -synucleinopathy, may be difficult due to the presence of common clinical features, as demonstrated by the relatively high rate of misdiagnosis at post-mortem evaluation⁴.

Previous studies suggested a role of different imaging techniques in aiding the differential diagnosis between PD and MSA. Atrophy on Magnetic Resonance Imaging (MRI) of putamen, middle cerebellar peduncle, pons, or cerebellum on conventional MRI and hypometabolism on FDG-PET in the putamen, middle cerebellar peduncle, pons, and cerebellum are already included as additional features for a diagnosis of possible MSA in the current diagnostic criteria¹. Moreover, it has been shown that suboptimal accuracy of neuroradiological diagnosis may be improved by the use of multimodal imaging approaches and advanced MRI techniques⁵.

So far, the ratio of the signal intensity of the T1-weighted and T2-weighted (T1w/T2w) MRI images, has been used as semi-quantitative measure for myelin content in gray matter⁶. Compared to other quantitative MRI techniques, it has the advantage that images can be easily acquired during routine clinical examination and without complex modeling of the MR signal, with high spatial resolution and sensitivity to neurodegenerative changes⁷⁻⁹.

In disorders with a strong demyelinating component (as e.g. in multiple sclerosis), the T1w/T2w ratio has been found to be lowered in pathologically vulnerable regions^{10,11}. However, recent studies have also pointed out on

¹Neuroscience Section, Department of Medicine, Surgery and Dentistry, Scuola Medica Salernitana, Center for Neurodegenerative Diseases (CEMAND), University of Salerno, 84131 Salerno, Italy. ²Neuroradiology Unit, Department of Neurosciences, University of Padua, Padua, Italy. ³Classe di Scienze Sperimentali, Scuola Superiore di Studi Universitari e Perfezionamento Sant'Anna, Pisa, Italy. ⁴Department of Advanced Medical and Surgical Sciences, University of Campania "Luigi Vanvitelli", Naples, Italy. ✉email: mpellecchia@unisa.it

	MSA (n = 26)	PD (n = 43)	HC (n = 56)	p
Age, ys (mean ± SD)	59.5 ± 6.7	64.3 ± 7.9	62.9 ± 9.1	ns
Gender (M/F)	15/11	26/17	34/22	ns
Disease duration, ys (mean ± SD)	3.6 ± 1.3	4.4 ± 2.4	–	ns
H&Y stage (mean ± SD)	2.5 ± 0.5	1.8 ± 0.54	–	ns
UPDRS-III (mean ± SD)	–	17.6 ± 9.6	–	
UMSARS-I (mean ± SD)	22.07 ± 6	–	–	
UMSARS-II (mean ± SD)	24.07 ± 6.9	–	–	
UMSARS-IV (mean ± SD)	2.7 ± 0.8	–	–	

Table 1. Demographic and clinical findings of enrolled subjects.

a different interpretation of the T1w/T2w ratio, suggesting that this measure may also reflect axon and dendrite density or iron content⁷. Consistently, increased T1w/T2w ratio has been recently found in the substantia nigra pars compacta of PD patients compared with healthy controls¹².

Since MSA-related pathology involves oligodendroglial and neuronal loss, with astroglial and microglial activation and increased iron content, in this study, we have performed a multimodal evaluation of tissue integrity by assessing both T1w/T2w ratio images and voxel-based morphometry (VBM) on gray and white matter (GM and WM) brain compartments. A multi-parameter analysis was performed with the aims of unveiling tissue damage in MSA patients as compared to healthy controls (HC) and PD patients and for assessing a new potential candidate MRI biomarker for differential diagnosis with PD.

Methods

Subjects. Twenty-six patients with probable MSA according to current diagnostic criteria [14 with the parkinsonian variant (MSA-P) and 12 with the cerebellar variant (MSA-C)], 43 patients with idiopathic PD and 56 healthy controls (HC) participated to the current study. Motor disability was assessed with the Unified MSA Rating Scale, part two (UMSARS-II) and the Unified PD Rating Scale, part three (UPDRS-III) in MSA and PD patients, respectively. In order to perform an additional exploratory analysis of clinico-radiological correlates in MSA, we also looked at specific items from the UMSARS I, and specifically we used item 1 to 6 total score for difficulties with daily activities, item 7 and 8 scores for walking difficulties and falls respectively, and item 8 to 12 total score for dysautonomia. Demographic and clinical data of enrolled subjects are reported in Table 1. The study was approved by the local Ethics committee—Comitato Etico Campania Sud—and all participants signed informed consent. The study was conducted in accordance with the Declaration of Helsinki principles.

MRI acquisition. All brain imaging data were acquired on a 3 T MRI scanner (MAGNETOM Skyra, Siemens, Erlangen Germany) operated with a 20-channel head and neck coil. The imaging protocol consisted of a 3D anatomical T1-weighted (T1w) Magnetization Prepared Rapid Gradient Echo (MPRAGE) sequence with repetition time (TR) = 2400 ms and echo time (TE) = 2.25 ms, spatial resolution = 1 × 1 × 1 mm³, matrix size = 256 × 256, anterior–posterior phase encoding direction, generalized autocalibrating partially parallel acquisitions (GRAPPA) factor of 2 in phase-encoding direction and a 3D T2-weighted (T2w) Sampling Perfection with Application optimized Contrast using different angle Evolutions (SPACE) sequence with TR = 3200, TE = 408 ms, variable flip angle, resolution = 1 × 1 × 1 mm³, matrix size = 256 × 256, anterior–posterior phase encoding direction, GRAPPA factor of 2 in phase-encoding⁹.

MRI data processing. For VBM analysis tissue probabilistic maps were obtained from T1w images and used to evaluate differences in terms of grey and white matter (GM and WM) atrophy. T1w native space images of each subject were segmented into GM and WM and normalized to MNI standard space using DARTEL algorithm¹³. Then the resulting tissue (GM/WM) probabilistic maps were modulated by the Jacobian determinants of the deformations to account for local compression and expansion due to linear and non-linear transformation¹⁴ and then smoothed with a Gaussian kernel of 6 mm FWHM. For the group analysis a group mask was created for each tissue, averaging and then binarizing with a threshold of 0.2 all the smoothed GM/WM maps of the HC subjects. Total intracranial volume (ICV) was also calculated for each subject as the sum of the three main brain tissue volumes (GM, WM and CSF).

In order to obtain semi-quantitative maps markers of myelin content, before the validated preprocessing⁶, T1w and T2w images were corrected for intensity nonuniformity with the bias correction tool implemented in the unified segmentation¹⁴ and available in SPM12. Then the T2w images were linearly registered to the T1w images using the FSL tool FLIRT^{15,16} for estimating and applying a rigid-body affine transformation with 6 degrees of freedom and cubic spline interpolation to minimize the WM and CSF contamination of GM voxels⁶. T1w/T2w maps were obtained using FSLMATHS to divide the T1w volumes by the corresponding aligned T2w ones. For the group analysis the DARTEL algorithm with the same group template and deformation fields as calculated for VBM analysis were used to normalize the T1w/T2w ratio maps to the standard MNI space. During the normalization procedure, T1w/T2w maps were smoothed with a Gaussian kernel of 6 mm FWHM.

Statistical analysis. The whole brain maps (GM and WM probability tissue maps and T1w/T2w ratio maps) were compared between groups in a voxel-based full factorial analysis as implemented in SPM12. Particularly a general linear model was used considering one factor of three levels for the group (MSA, PD, HC) and two (age and sex) and three (age, sex and ICV) covariate factors respectively for T1w/T2w and GM or WM analyses. Voxels were considered significant with $p < 0.05$ after family-wise error correction (FWE) for multiple comparisons as implemented in SPM12.

A post-hoc regional analysis was also performed by extracting the mean parameter values (GM and WM probability and T1w/T2w ratio) in the voxels of detected differences in the voxel-based analysis and in the substantia nigra pars compacta (SN) individuated using masks freely available at <https://github.com/apoorvasafi/NMS-SNc-atlas>. The regional values were compared between groups (MSA, PD, HC) and MSA subgroups (MSA-C, MSA-P) with a two-sample t-test after correcting for age with linear regression.

Receiver operating characteristic (ROC) curve analysis was then performed to evaluate the ability of the MRI parameters to discriminate between MSA and HC, MSA and PD and MSA-P and PD. For this analysis, a generalized linear model with binomial distribution and logit link function as setting parameters was first computed on the regional values of GM or WM and T1w/T2w. For each ROI, the ROC curve was calculated on the obtained predictive values, allowing to calculate the corresponding area under the curve (AUC), confidence interval, and p -values. The optimal cutoff point (and corresponding sensitivity and specificity) was determined using the Youden method.

Correlations between MRI parameters and clinical variables were checked with the Spearman's rank correlation coefficient both considering the whole MSA group and the subgroups (MSA-P and MSA-C); a 5% level of significance was used for all tests.

Results

The three groups did not differ in age and sex distribution (Table 1). Patients with MSA and PD had similar disease duration (Table 1). Disease severity, as assessed by UPDRS-III and UMSARS, is reported in Table 1.

Compared to HC, MSA patients showed reduced GM volume in bilateral putamen (left cluster size = 128 voxels, right cluster size = 1143 voxels) and in an extended cluster in the cerebellar gray matter (cluster size = 379,270 voxels) (Fig. 1a). When comparing MSA versus PD patients, the former showed reduced GM volume in two clusters of bilateral putamen (left cluster size = 119 voxels, right cluster size = 749 voxels) and in an extended area of the cerebellar gray matter (cluster size = 134,350 voxels) (Fig. 1b). No significant differences were detected when comparing PD versus HC. Post-hoc regional analyses displayed significant between-group differences, between MSA-P and both PD and HC, and between MSA-C and both PD and HC (Fig. 1c).

Compared to HC, MSA patients showed reduced WM volume in a cluster extending from the cerebellar WM to the brainstem (cluster size = 413,700 voxels, Fig. 2a). When compared to PD patients, MSA showed a WM volume reduction in a cluster extending from the cerebellar WM to the brainstem (cluster size = 257,580 voxels, Fig. 2b). No significant differences were detected when comparing PD versus HC. Regional post-hoc analyses showed a significant difference in WM atrophy of the cerebellum/brainstem cluster between MSA-P and both PD and HC and between MSA-C and both PD and HC (Fig. 2c). Regional analysis on SN revealed significant differences in left SN between HC and MSA (HC vs MSA-C, $p < 0.001$; HC vs MSA-P, $p = 0.017$), and between PD and MSA (PD vs MSA-C, $p < 0.001$; PD vs MSA-P, $p = 0.018$). Significant differences were also detected in right SN between HC and MSA (HC vs MSA-C, $p < 0.001$; HC vs MSA-P, $p = 0.008$), and between PD and MSA (PD vs MSA-C, $p < 0.001$; PD vs MSA-P, $p = 0.005$), see Supplementary Fig. 1.

Four HC, 1 PD and 3 MSA patients were excluded from the T1w/T2w imaging analysis due to missing 3D T2w series.

Whole brain voxel-based comparison of T1w/T2w maps did not show any difference between groups. Nonetheless, regional post-hoc analysis in the aforementioned clusters of GM or WM atrophy showed significant differences between MSA-P and HC and between MSA-P and PD in the right and left putamen, with increased T1w/T2w values in the MSA-P subgroup (see Fig. 3b, c). No significant differences in terms of T1w/T2w values were detected in the clusters of GM atrophy in the cerebellum and WM atrophy in the cerebellum/brainstem (Fig. 3a, d). The analysis on regional T1w/T2w mean values in SN disclosed a significant difference between HC and MSA-C subgroup ($p = 0.01$) for left SN and a significant difference between HC and PD ($p = 0.03$) and HC and MSA-C subgroup ($p < 0.001$) in right SN, see Supplementary Fig. 1.

Regional values in significantly different clusters were also used for discriminant analysis between groups by using both T1w/T2w parameters and combined GM or WM with T1w/T2w.

T1w/T2w value in the left putamen discriminated MSA versus HC, and MSA versus PD, but not MSA-P versus PD. T1w/T2w value in the right putamen discriminated MSA versus HC and MSA versus PD, but not MSA-P versus PD. T1w/T2w value in left and right SN discriminated significantly between MSA and HC groups.

Combination of regional GM and T1w/T2w in the cerebellum significantly discriminated MSA from HC and MSA from PD, but not MSA-P from PD. The multi-parameter (multi-variate) combination of regional GM and T1w/T2w in the left putamen significantly discriminated MSA from HC, MSA from PD and MSA-P from PD. The multi-parameter (multi-variate) combination of regional GM and T1w/T2w in the right putamen significantly discriminated MSA from HC, MSA from PD, and MSA-P from PD. The multi-parameter (multi-variate) combination of regional WM and T1w/T2w in the cerebellum/brainstem significantly discriminated MSA from HC, MSA from PD, but not MSA-P from PD. Additionally the combination of WM and T1w/T2w regionally in left and right SN allows to significantly discriminate between MSA and HC, MSA and PD and MSA-C subgroup and PD. The detailed results of the ROC analysis (AUC, sensitivity, specificity and p -values) are summarized in Table 2.

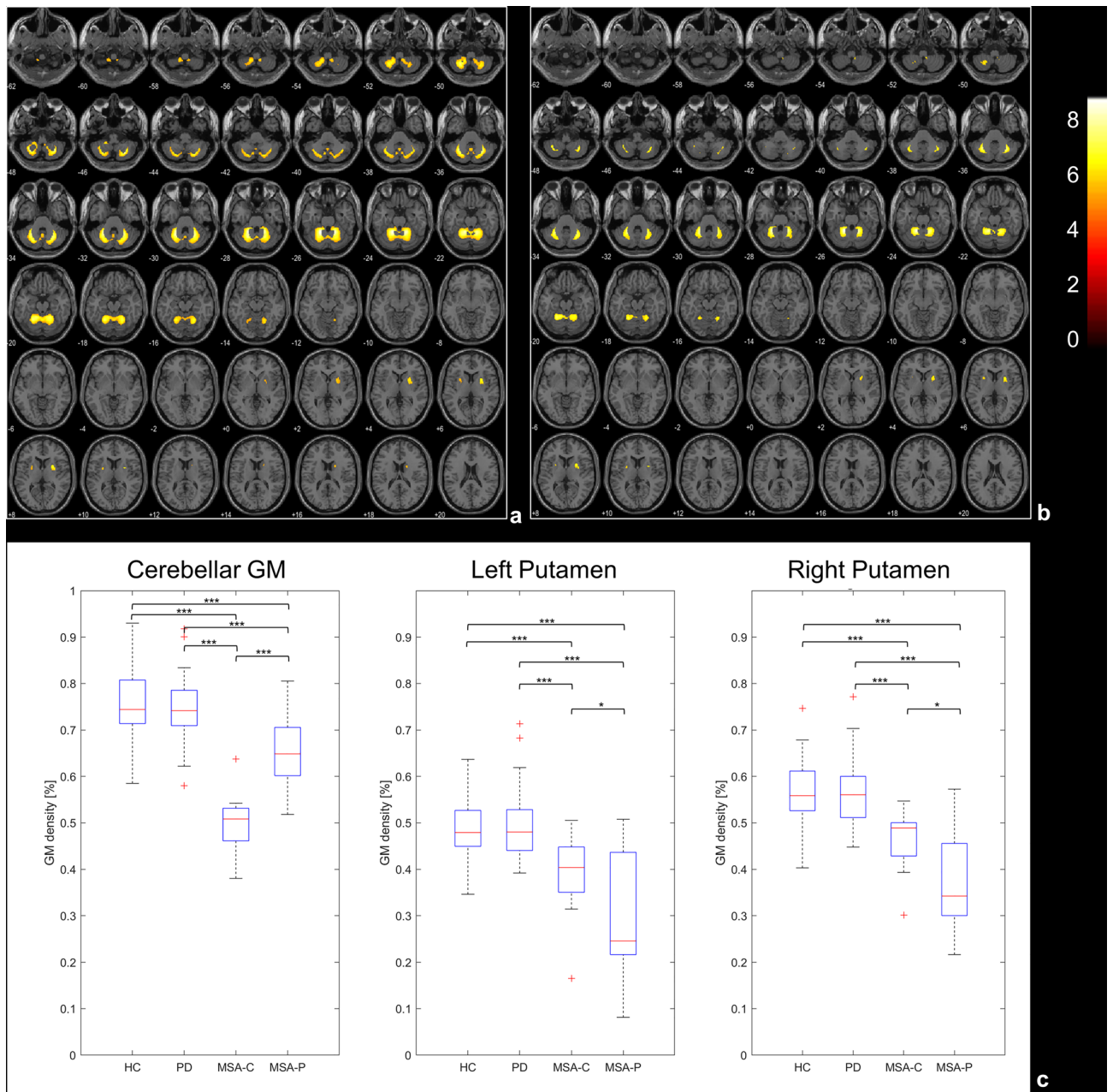


Figure 1. Upper panel t-maps of the voxel-wise GM comparisons respectively between HC and MSA (a) and PD and MSA (b). Statistical threshold is set to $p < 0.05$ after FWE correction for multiple comparison. Lower panel box-plots of the GM density distribution in the significant clusters (from the comparison HC vs MSA) for each group, and results of the post-hoc t-tests on the regional values (c). * $p < 0.05$, ** $p < 0.01$, *** $p < 0.001$.

After correcting regional GM or WM tissue density for age and sex, residual GM volume in left and right Putamen was significantly correlated with the UMSARS falling score in all the MSA group (left: $\rho = -0.379$, $p = 0.05$; right $\rho = -0.511$, $p = 0.008$). Only in MSA-P patients residual GM volume in the cerebellum/brainstem was significantly correlated with UMSARS-II ($\rho = -0.515$, $p = 0.05$) and UMSARS falling score ($\rho = -0.529$, $p = 0.05$) while residual WM volume in the cerebellum/brainstem was significantly correlated with UMSARS-I ($\rho = -0.560$, $p = 0.037$), UMSARS-II ($\rho = -0.537$, $p = 0.047$), UMSARS walking ($\rho = -0.544$, $p = 0.044$) and UMSARS falling ($\rho = -0.645$, $p = 0.013$) scores. Regional WM density in bilateral SN was significantly correlated to UMSARS walking score (left: $\rho = -0.631$, $p = 0.015$; right $\rho = -0.593$, $p = 0.025$) and UMSARS falling score (left: $\rho = -0.573$, $p = 0.032$; right $\rho = -0.550$, $p = 0.041$) only in the MSA-P subgroup. After correcting T1w/T2w regional values for age and sex, significant correlations were found between UMSARS autonomic score and regional value in left SN ($\rho = -0.776$, $p = 0.0049$) only in the MSA-P subgroup. None of the correlations resulted significant after correction for multiple comparisons.

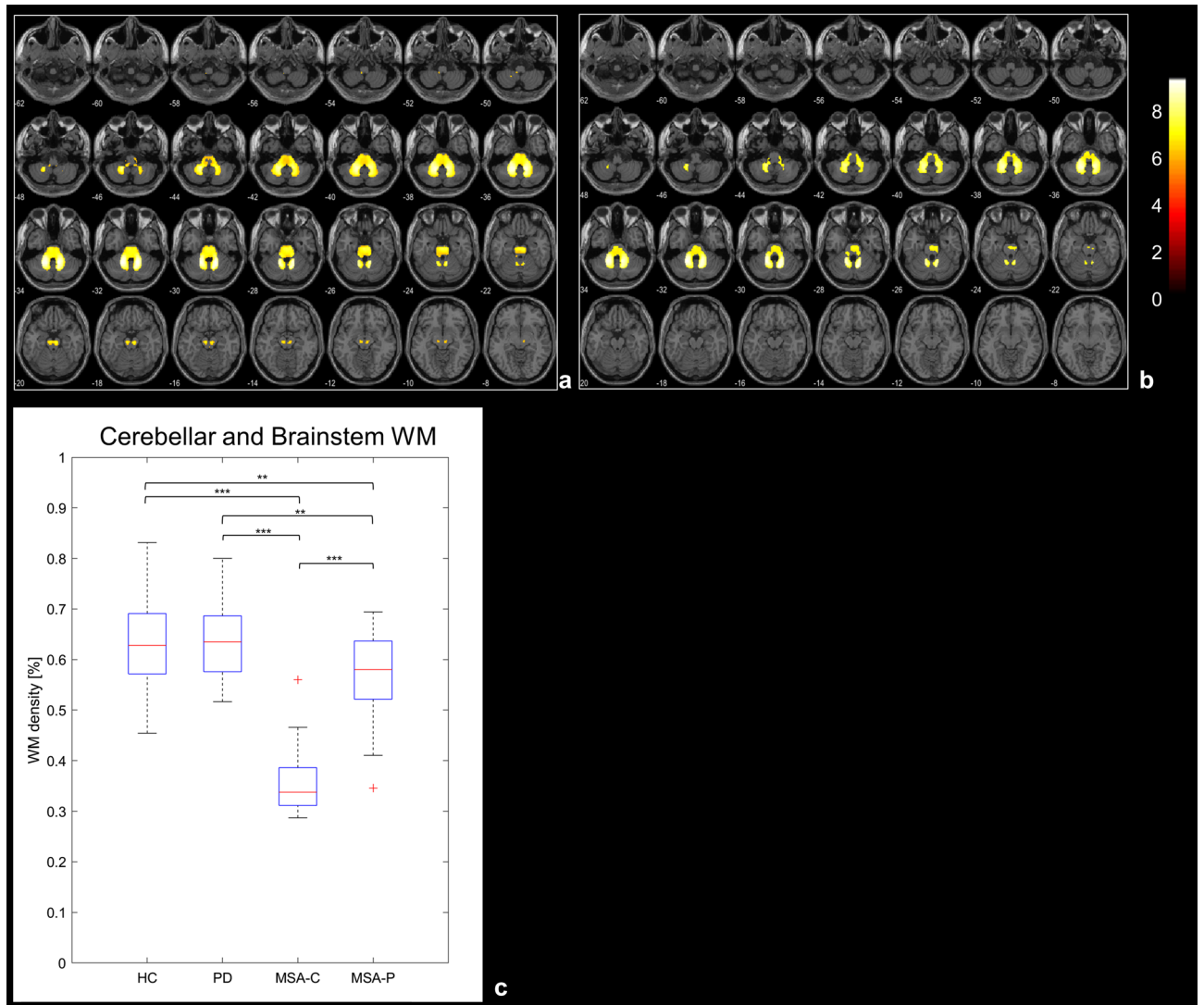


Figure 2. Upper panel t-maps of the voxel-wise WM comparisons respectively between HC and MSA (a) and PD and MSA (b). Statistical threshold is set to $p < 0.05$ after FWE correction for multiple comparison. Lower panel box-plots of the WM density distribution in the significant cluster (from the comparison HC vs MSA) for each group, and results of the post-hoc t-tests on the regional values. * $p < 0.05$, ** $p < 0.01$, *** $p < 0.001$.

Discussion

In this study we performed a multi-parametric evaluation of tissue integrity assessing both T1w/T2w ratio images and voxel-based morphometry on GM and WM tissue density to investigate whole brain damage in MSA patients as compared to PD patients and HC and evaluate a potential semi-quantitative biomarker for differential diagnosis with PD.

As expected, we found MSA patients to have GM atrophy in bilateral putamen and cerebellum and WM atrophy in the cerebellum/brainstem compared to both PD patients and HC. Post-hoc regional analysis showed that MSA patients had significant bilateral atrophy of SN pars compacta as compared to both PD and HC. This finding is consistent with neuropathological findings of MSA³ and previous VBM data on gray matter atrophy in dorsal midbrain¹⁷, but in our study we first obtained a semiquantitative assessment of regional tissue density in the SN of MSA patients considering WM density and T1w/T2w values.

On the other hand, T1w/T2w changes did not strictly parallel the obtained atrophy patterns, with MSA and PD patients showing similar values in the cerebellum/brainstem, but MSA-P showing a significant increase in T1w/T2w values in both right and left putamen as compared to PD and HC. Moreover, T1w/T2w regional mean value in bilateral SN pars compacta was found to be higher in MSA-C patients compared to HC, suggesting that T1w/T2w ratios deserve to be further studied as an MRI biomarker in both MSA subtypes. Additionally, T1w/T2w regional mean value in the right SN was found to be higher in PD patients compared to HC, confirming recent evidence in PD patients¹². The combined use of regional GM and T1w/T2w values in the right and left putamen showed the highest accuracy in discriminating MSA-P from PD, while the combined use of the same parameters showed a good accuracy in discriminating MSA from both PD and HC. A similar good accuracy was also found in discriminating MSA from PD and HC by either combining regional GM and T1w/T2w values in

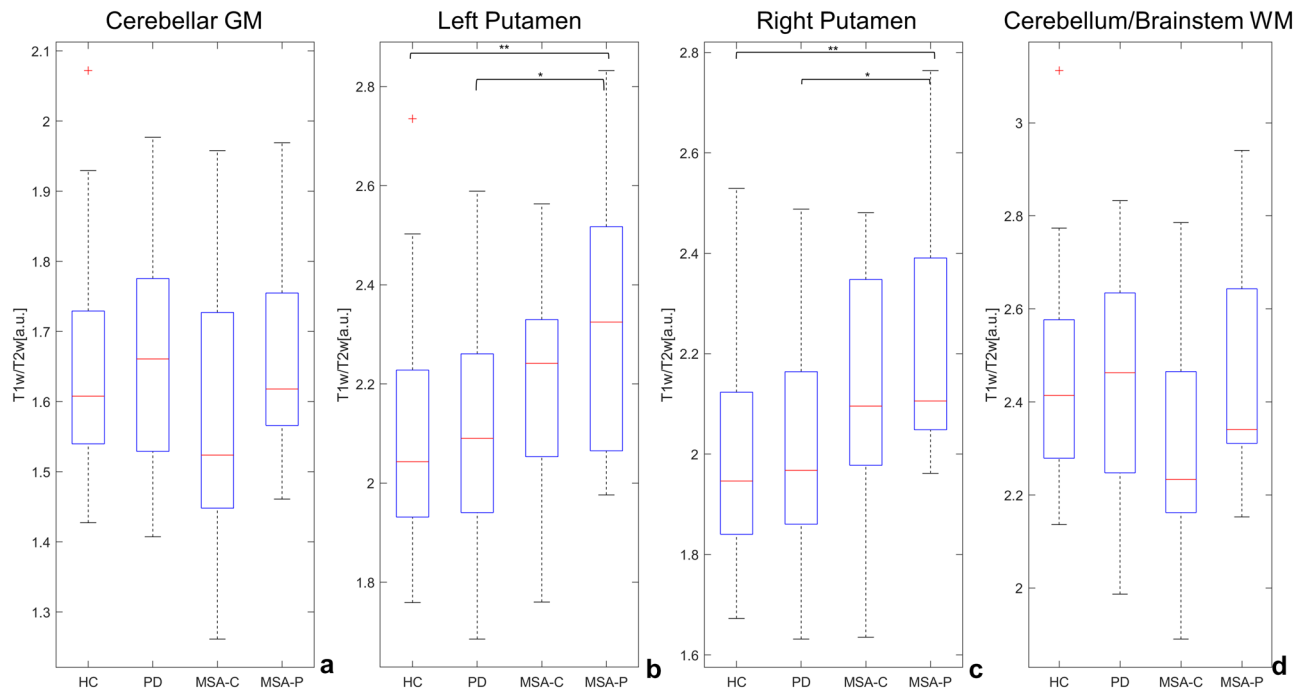


Figure 3. Box-plots of the T1w/T2w distribution in the significant clusters (from the comparison HC vs MSA in GM and WM) for each group, and results of the post-hoc t-tests on the regional values. * $p < 0.05$, ** $p < 0.01$.

the cerebellum or regional WM and T1w/T2w in the cerebellum and brainstem. Finally, a quite good accuracy was found in discriminating MSA from PD and HC, and MSA-C from PD by combining regional tissue density and T1w/T2w values in both left and right SN.

The higher degree of putaminal and cerebellar gray matter atrophy of MSA patients largely confirm previous results^{17–19} and is in keeping with the evidence of MSA being a more aggressive and widespread disorder than PD. We also found a significant WM volume reduction in a cluster extending from the cerebellum to the brainstem in both MSA-P and MSA-C versus PD and HC. Consistently, few previous studies have already described WM atrophy in brainstem and cerebellum in MSA-C and MSA-P patients as compared to HC^{20–22}. In patients with PD we found no differences in terms of atrophy when compared to HC, which is also in line with previous results obtained in patients with similar disease duration²³.

Previous studies have used the T1w/T2w ratio to detect cortical changes in patients with multiple sclerosis, showing lower values in pathologically vulnerable regions^{10,11}.

On the other hand, higher cortical values of the T1w/T2w ratio have been found in Alzheimer's disease²⁴ and Huntington's disease²⁵ as compared to HC, and a similar finding has been reported in a subcortical structure, namely substantia nigra pars compacta, in PD patients compared to HC¹². Decrease in neuronal density, resulting in higher myelin proportions, or iron accumulation have been suggested to account for such previous results²⁵ and may also account for the increased T1w/T2w ratio found in the atrophic putamen of our MSA-P patients. Indeed, putaminal diffusivity changes have been reported corresponding to prominent neuronal loss²⁶, and quantitative susceptibility mapping has confirmed increased iron deposition in the putamen of MSA-P patients^{27,28}.

More recently, a reduced T1w/T2w ratio in the medium cerebellar peduncle has been reported in MSA-C compared to HC²⁹, suggesting that this measure can also be useful as a quantitative biomarker of myelin loss. Indeed, this measure was also found to be correlated with the ICARS score in early MSA-C but, consistently with our results, not with UMSARS part 2 scores, possibly due to the inadequacy of the latter scale that was originally developed to characterize cerebellar ataxia and parkinsonism²⁹. There are, however, some important conceptual and methodological differences between this study and ours: in fact, differently from the previous study, we adhered to the original protocol described to assess T1w/T2w ratio⁶, using 3D acquisition schemes and 1 mm³ spatial resolution in both T1w and T2w images acquisition. This protocol was specifically developed to analyze the entire brain, i.e., without prior assumptions on the potentially affected regions. To this more general purpose, we combined the T1w/T2w analysis with a classical VBM analysis at the same (typical) resolution of morphometric studies at 3 Tesla.

We found that UMSARS motor scores in MSA-P patients were worse in patients with greater GM and WM atrophy in the cerebellum/brainstem and, similarly, UMSARS functional scores were worse in patients with greater WM atrophy in the cerebellum/brainstem. We can speculate that correlations with such clinical parameters may reflect the progressive brainstem/cerebellar involvement during the course of MSA-P. Consistently, a similar relationship between UMSARS motor scores and cerebellar atrophy in MSA-P patients has been reported in a previous VBM study, also failing to show relationships between UMSARS scores and putaminal atrophy³⁰. By looking at specific items from the UMSARS I, higher falling scores were related with bilateral putaminal atrophy in the whole MSA group, greater GM and WM atrophy in the cerebellum/brainstem only in MSA-P patients and greater WM atrophy in the SN. Moreover, greater impairment in walking was associated with greater WM

	T1w/T2w				T1w/T2w+ Tissue density (GM or WM)			
	AUC	<i>p</i>	Sensitivity	Specificity	AUC	<i>p</i>	Sensitivity	Specificity
MSA vs HC								
L-Putamen	0.70	0.005	0.87	0.46	0.84	<0.001	0.74	0.83
R-Putamen	0.71	0.003	0.91	0.50	0.88	<0.001	0.78	0.87
Cerebellum GM	0.54	>0.05	0.30	0.88	0.93	<0.001	0.78	0.96
Brainstem WM	0.60	>0.05	0.65	0.62	0.88	<0.001	0.83	0.75
L-SN	0.72	<0.001	0.61	0.77	0.88	<0.001	0.96	0.71
R-SN	0.76	<0.001	0.87	0.60	0.90	<0.001	0.96	0.77
MSA vs PD								
L-Putamen	0.67	0.019	0.52	0.81	0.78	<0.001	0.57	0.92
R-Putamen	0.68	0.010	0.83	0.56	0.83	<0.001	0.78	0.83
Cerebellum GM	0.57	>0.05	0.48	0.56	0.85	<0.001	0.74	0.98
Brainstem WM	0.59	>0.05	0.52	0.65	0.81	<0.001	0.61	0.90
L-SN	0.63	>0.05	0.43	0.87	0.79	<0.001	0.96	0.62
R-SN	0.64	>0.05	0.26	0.94	0.80	<0.001	0.65	0.90
MSA-P vs PD								
L-Putamen	0.72	>0.05	0.30	0.92	0.89	0.01	0.22	1
R-Putamen	0.66	>0.05	0.57	0.63	0.93	<0.001	0.26	1
Cerebellum GM	0.40	>0.05	0.52	0.52	0.68	>0.05	0.78	0.88
Brainstem WM	0.35	>0.05	0.70	0.44	0.61	>0.05	0.39	1
L-SN	0.62	>0.05	0.57	0.81	0.78	>0.05	0.48	0.94
R-SN	0.45	>0.05	0.87	0.58	0.76	>0.05	0.61	0.92
MSA-C vs PD								
L-Putamen	0.50	>0.05	0.52	0.75	0.59	>0.05	0.83	0.58
R-Putamen	0.48	>0.05	0.17	0.98	0.65	>0.05	0.78	0.87
Cerebellum GM	0.68	>0.05	0.13	0.92	0.92	<0.001	0.57	1
Brainstem WM	0.76	0.018	0.26	0.88	0.93	<0.001	0.48	1
L-SN	0.62	>0.05	0.26	0.92	0.84	<0.001	0.52	0.87
R-SN	0.66	>0.05	0.22	0.96	0.84	<0.001	0.52	0.94

Table 2. ROC analysis results. ROC analysis results for patients' discrimination. T1w/T2w regional values were used to discriminate between groups both alone and in combination with mean regional tissue density (GM/WM). Significant results were enhanced in bold.

atrophy in the cerebellum/brainstem and bilateral SN only in MSA-P patients. Indeed, none of such correlations with specific UMSARS items survived after correction for multiple comparisons, due to the great number of variables examined, nonetheless these functional correlates may be of interest for future studies. We must acknowledge that evaluating our MSA patients also with UPDRS and an ataxia specific scale would have been desirable to better evaluate relationships with MRI parameters.

Further validation of the T1w/T2w ratio in MSA is needed to establish if this measure alone or combined with other validated MRI parameters can be useful as a quantitative MRI biomarker for differential diagnosis and follow-up of MSA patients.

Received: 8 July 2021; Accepted: 22 October 2021

Published online: 04 November 2021

References

- Gilman, S. *et al.* Second consensus statement on the diagnosis of multiple system atrophy. *Neurology* **71**, 670–676 (2008).
- Ubhi, K., Low, P. A. & Masliah, E. Multiple system atrophy: A clinical and neuropathological perspective. *Trends Neurosci.* **34**, 581–590 (2011).
- Jellinger, K. Neuropathology. In *Multiple System Atrophy* (ed. Wenning, G. K.) 17–56 (Springer Verlag, 2014).
- Koga, S. *et al.* When DLB, PD and PSP masquerade as MSA: An autopsy study of 134 patients. *Neurology* **85**, 404–412 (2015).
- Stankovic, I. *et al.* A critique of the second consensus criteria for multiple system atrophy. *Mov. Disord.* **34**, 975–984 (2019).
- Glasser, M. F. & Van Essen, D. C. Mapping human cortical areas in vivo based on myelin content as revealed by T1- and T2-weighted MRI. *J. Neurosci.* **31**, 11597–11616 (2011).
- Arshad, M., Stanley, J. A. & Raz, N. Test–retest reliability and concurrent validity of in vivo myelin content indices: Myelin water fraction and calibrated T1w/T2w image ratio. *Hum. Brain Mapp.* **38**, 1780–1790 (2017).
- Grydeland, H., Walhovd, K. B., Tamnes, C. K., Westlye, L. T. & Fjell, A. M. Intracortical myelin links with performance variability across the human lifespan: Results from T1- and T2-weighted MRI myelin mapping and diffusion tensor imaging. *J. Neurosci.* **33**, 18618–18630 (2013).

9. Canna, A. *et al.* A group-level comparison of volumetric and combined volumetric-surface normalization for whole brain analyses of myelin and iron maps. *Magn. Reson. Imaging* **54**, 225–240 (2018).
10. Beer, A. *et al.* Tissue damage within normal appearing white matter in early multiple sclerosis: Assessment by the ratio of T1- and T2-weighted MR image intensity. *J. Neurol.* **263**, 1495–1502 (2016).
11. Nakamura, K., Chen, J. T., Ontaneda, D., Fox, R. J. & Trapp, B. D. T1-/T2-weighted ratio differs in demyelinated cortex in multiple sclerosis. *Ann. Neurol.* **82**, 635–639 (2017).
12. Du, G., Lewis, M. M., Sica, C., Kong, L. & Huang, X. Magnetic resonance T1w/T2w ratio: A parsimonious marker for Parkinson's disease. *Ann. Neurol.* **85**, 96–104 (2019).
13. Ashburner, J. A fast diffeomorphic image registration algorithm. *Neuroimage* **38**, 95–113 (2007).
14. Good, C. D. *et al.* A voxel-based morphometric study of ageing in 465 normal adult human brains. *Neuroimage* **14**, 21–36 (2001).
15. Ashburner, J. & Friston, K. J. Unified segmentation. *Neuroimage* **26**, 839–851 (2005).
16. Jenkinson, M. Improved optimization for the robust and accurate linear registration and motion correction of brain images. *Neuroimage* **17**, 825–841 (2002).
17. Minnerop, M. *et al.* Voxel-based morphometry and voxel-based relaxometry in multiple system atrophy—A comparison between clinical subtypes and correlations with clinical parameters. *Neuroimage* **36**, 1086–1095 (2007).
18. Shao, N., Yang, J. & Shang, H. Voxelwise meta-analysis of gray matter anomalies in Parkinson variant of multiple system atrophy and Parkinson's disease using anatomic likelihood estimation. *Neurosci. Lett.* **587**, 79–86 (2015).
19. Lin, J., Xu, X., Hou, Y., Yang, J. & Shang, H. Voxel-based meta-analysis of gray matter abnormalities in multiple system atrophy. *Front. Aging Neurosci.* **12**, 1–12 (2020).
20. Specht, K., Minnerop, M., Müller-Hubenthal, J. & Klockgether, T. Voxel-based analysis of multiple system atrophy of cerebellar type: Complementary results by combining voxel-based morphometry and voxel-based relaxometry. *Neuroimage* **25**, 287–293 (2005).
21. Shigemoto, Y. *et al.* In vivo evaluation of gray and white matter volume loss in the Parkinsonian variant of multiple system atrophy using SPM8 plus DARTEL for VBM. *NeuroImage Clin.* **2**, 491–496 (2013).
22. Faber, J. *et al.* Prominent white matter involvement in multiple system atrophy of cerebellar type. *Mov. Disord.* **35**, 816–824 (2020).
23. Pan, P. L., Song, W. & Shang, H. F. Voxel-wise meta-analysis of gray matter abnormalities in idiopathic Parkinson's disease. *Eur. J. Neurol.* **19**, 199–206 (2012).
24. Pelkmans, W. *et al.* Gray matter T1-w/T2-w ratios are higher in Alzheimer's disease. *Hum. Brain Mapp.* **40**, 3900–3909 (2019).
25. Rowley, C. D. *et al.* Altered intracortical T1-weighted/T2-weighted ratio signal in Huntington's disease. *Front. Neurosci.* **12**, 1–9 (2018).
26. Bajaj, S. *et al.* Diffusion-weighted MRI distinguishes Parkinson disease from the parkinsonian variant of multiple system atrophy: A systematic review and meta-analysis. *PLoS ONE* **12**, e0189897 (2017).
27. Mazzucchi, S. *et al.* Quantitative susceptibility mapping in atypical parkinsonisms. *NeuroImage Clin.* **24**, 101999 (2019).
28. Sjöström, H., Granberg, T., Westman, E. & Svenningsson, P. Quantitative susceptibility mapping differentiates between parkinsonian disorders. *Parkinsonism Relat. Disord.* **44**, 51–57 (2017).
29. Sugiyama, A., Yokota, H. & Hirano, S. Magnetic resonance T1w/T2w ratio in the middle cerebellar peduncle might be a sensitive biomarker for multiple system atrophy. *Eur. Radiol.* **31**, 4277–4284 (2021).
30. Tsuda, M., Asano, S., Kato, Y., Murai, K. & Miyazaki, M. Differential diagnosis of multiple system atrophy with predominant parkinsonism and Parkinson's disease using neural networks. *J. Neurol. Sci.* **401**, 19–26 (2019).

Author contributions

S.P. performed MRI data processing and analysis and wrote the first draft of the paper. R.M., G.D.S., F.D.S. and F.E. critically revised MRI analyses and the final version of the paper. M.C.R., R.E., M.P., P.B. collected clinical data and critically revised the final version of the paper. M.T.P. collected clinical data and wrote the final version of the paper.

Competing interests

The authors declare no competing interests.

Additional information

Supplementary Information The online version contains supplementary material available at <https://doi.org/10.1038/s41598-021-01222-5>.

Correspondence and requests for materials should be addressed to M.T.P.

Reprints and permissions information is available at www.nature.com/reprints.

Publisher's note Springer Nature remains neutral with regard to jurisdictional claims in published maps and institutional affiliations.



Open Access This article is licensed under a Creative Commons Attribution 4.0 International License, which permits use, sharing, adaptation, distribution and reproduction in any medium or format, as long as you give appropriate credit to the original author(s) and the source, provide a link to the Creative Commons licence, and indicate if changes were made. The images or other third party material in this article are included in the article's Creative Commons licence, unless indicated otherwise in a credit line to the material. If material is not included in the article's Creative Commons licence and your intended use is not permitted by statutory regulation or exceeds the permitted use, you will need to obtain permission directly from the copyright holder. To view a copy of this licence, visit <http://creativecommons.org/licenses/by/4.0/>.

© The Author(s) 2021